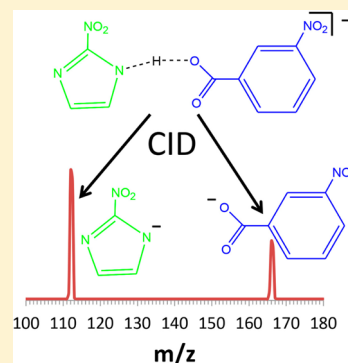


Gas-Phase Acidities of Nitrated Azoles as Determined by the Extended Kinetic Method and Computations

Charles M. Nichols, William M. Old, W. Carl Lineberger, and Veronica M. Bierbaum*

Department of Chemistry and Biochemistry, JILA, University of Colorado, Boulder, Colorado 80309, United States

ABSTRACT: Making use of the extended kinetic method and the alternative method for data analysis, we have experimentally determined $\Delta H^\circ_{\text{acid}}$ (kcal/mol) for six mononitrated azole species (2-nitropyrrole = 337.0, 3-nitropyrrole = 335.8, 3-nitropyrazole = 330.5, 4-nitropyrrole = 329.5, 2-nitroimidazole = 327.4, and 4-nitroimidazole = 325.0). We report an absolute uncertainty of ± 2.2 kcal/mol that arises from the uncertainties of the reference acids; the relative values are known within 0.4 kcal/mol. Combining these experimental $\Delta H^\circ_{\text{acid}}$ values with $\Delta S^\circ_{\text{acid}}$ values calculated at the B3LYP/aug-cc-pVTZ level of theory, we report $\Delta G^\circ_{\text{acid}}$ (kcal/mol) for the nitroazoles (2-nitropyrrole = 329.4, 3-nitropyrrole = 328.4, 3-nitropyrazole = 323.1, 4-nitropyrrole = 322.0, 2-nitroimidazole = 319.7, and 4-nitroimidazole = 317.6); the absolute uncertainties are ± 2.4 kcal/mol. In addition to the experimental studies, we have computationally investigated the gas-phase acidities and electron affinities of the azoles in this work, as well as higher-order aza- and dinitro-substituted azoles. We discuss trends in the stabilities of the deprotonated azoles based on aza substitution and nitro group placement. 4-Nitroimidazole has already found use as the anionic component in ionic liquids, and we propose that the additional nitrated azolate ions are potential candidates for the anionic component of ionic liquids.



INTRODUCTION

Azoles, five-membered aromatic rings in which one or more CH is replaced by N, are important organic compounds relevant to biological and material sciences. Pyrrole and imidazole, two of the simplest azoles, are found naturally as components of the amino acids tryptophan and histidine, the nucleobases adenine and guanine, and heme B. Because of the strong electron donor interaction of the nitrogen atoms, pyrrole and imidazole are known to coordinate with metal ions as stable ligands.¹ Furthermore, azole compounds are ubiquitous components of ionic liquids. Although ionic liquids have been known for over 100 years,² there has been a resurgence of interest in their application and characterization. These compounds are unusual because their melting point is ≤ 100 °C. This property has led to the use of ionic liquids as reusable green solvents because of their low vapor pressure.³ Because of their stability, these compounds are finding use as novel electrolytic compounds in batteries, capacitors, and solar cells.^{4,5} Additionally, ionic liquids are under study for use as a next-generation hypergolic fuel⁶ and as the ionic medium in ion thrusters.⁷ In some cases, modified azole compounds have found use as both the cationic and anionic species in ionic liquids.^{8,9} For example, 4-nitroimidazolate, an anion studied herein, has been combined with 1-butyl-3-methylimidazolium to produce a compound that melts at -63 °C and is thermally stable to 185 °C.⁹ In this work, we examine the gas-phase acidity of several nitrated azoles in an effort to characterize the stability of their conjugate bases, i.e., their corresponding anions. The nitrated molecules of this study, illustrated in Figure 1 below the parent azoles, vary by the placement of the ring-nitrogen atom as well as the placement of the nitro group.

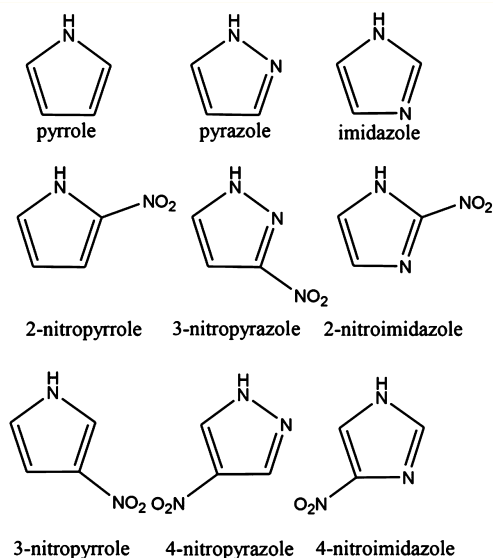


Figure 1. Selected azoles and their nitrated derivatives. The acidic hydrogen is indicated on the pertinent nitrogen atom.

The gas-phase acidity of molecules is of fundamental interest to many chemists. This property reflects the intrinsic stabilities of molecules and their deprotonated anions. It is common practice to determine the acidity of molecules by relative methods that compare a molecule of unknown acidity to one

Received: November 4, 2014

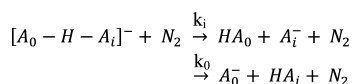
Revised: December 11, 2014

Published: December 18, 2014

for which the acidity has been previously determined. Several mass-spectrometry approaches are used to study the relative gas-phase acidities of molecules including proton-transfer equilibrium,^{10–16} bracketing,^{17,18} and the kinetic method.^{19–28} Historically, our lab has used the flowing afterglow-selected ion flow tube (FA-SIFT) to determine the gas-phase acidity of molecules.^{14–17} However, we were not able to use the FA-SIFT for this study because both the nitroazoles and the reference organic acids are not sufficiently volatile. Instead, we employed Cooks' kinetic method²⁰ and a triple quadrupole instrument to determine the gas-phase acidities of the nitrated azoles.

The kinetic method is a competitive dissociation technique that examines the relative proton affinity of two anions (gas-phase acidity) or two neutrals (proton affinity). The technique monitors the collision-induced fragmentation of anionic proton-bound heterodimers (Scheme 1).

Scheme 1. Competitive Dissociation of Anionic Proton-Bound Heterodimers



In Scheme 1, HA_i represents a series of reference acids with known gas-phase acidities and HA_0 represents a compound of unknown acidity. The ratio of the intensities of the two product ions (A_i^- and A_0^-) is directly related to the ratio of the two rate constants (k_i and k_0). N_2 is the collision gas used for this experiment.

The kinetic method has been used extensively over the last 20 years. The extended kinetic method, an improvement over Cooks' standard method,²⁰ was introduced by Fenselau and co-workers.²³ This approach requires that the reference acids are functionally similar among themselves but different from the unknown acid under investigation. This allows the assumption that the entropic contributions for proton transfer between the unknown and reference acid anions are constant [$\Delta\Delta S^\circ(HA_0, HA_i) = \Delta S^\circ_{\text{acid}}(HA_i) - \Delta S^\circ_{\text{acid}}(HA_0) \approx \text{constant}$]. This assumption becomes a good approximation when the reference acids are thoughtfully chosen to be similar in structure as well as functionality. The extended kinetic method also requires that the tandem mass spectrometry experiments are performed over multiple collision activation conditions. To perform the analysis, the logarithms of the ratio of the two rate constants, $\ln(k_i/k_0)$, in Scheme 1 are plotted against the proton affinities of the reference anions, $\Delta H^\circ_{\text{acid}}(HA_i)$. This provides the following relationship:

$$\ln \frac{[A_i^-]}{[A_0^-]} \approx \ln \frac{k_i}{k_0} \approx -\frac{\Delta H^\circ_{\text{acid}}(HA_i)}{RT_{\text{eff}}} + \frac{GA^{\text{app}}(HA_0)}{RT_{\text{eff}}} \quad (1)$$

In eq 1, the apparent gas-phase acidity term, GA^{app} , is the analogue of the apparent gas-phase basicity introduced by Wesdemiotis and co-workers.²⁴ At the x -intercept (where the ratio of $k_i/k_0 = 1$), $GA^{\text{app}}(HA_0) = \Delta H^\circ_{\text{acid}}(HA_i)$. The effective temperature (T_{eff}) represents the internal energy of the collisionally activated heterodimer. It is not a true thermodynamic temperature but rather a measure of the distribution of the energy available to the dimer.^{22,29,30} When $\ln([A_i^-]/[A_0^-])$ is plotted against $\Delta H^\circ_{\text{acid}}(HA_i)$, a linear regression is obtained with slope equal to $1/RT_{\text{eff}}$. Each unique collision activation condition provides a characteristic T_{eff} and $GA^{\text{app}}(HA_0)$.

Because the extended kinetic method requires the use of multiple activation conditions, multiple T_{eff} and $GA^{\text{app}}(HA_0)$ values are obtained. The $GA^{\text{app}}(HA_0)$ values are then plotted versus T_{eff} using the following relationship:

$$GA^{\text{app}}(HA_0) = \Delta H^\circ_{\text{acid}}(HA_0) - T_{\text{eff}} \Delta\Delta S^\circ(HA_0, HA_i) \quad (2)$$

For eq 2, $\Delta\Delta S^\circ(HA_0, HA_i)$ is provided by the slope of the line, while determination of the y -intercept gives $\Delta H^\circ_{\text{acid}}(HA_0)$. This two-plot technique for determining $\Delta H^\circ_{\text{acid}}(HA_0)$ was first introduced by Armentrout²⁵ as the "alternative method".

More recently, another method for analyzing extended kinetic method data, called the orthogonal distance regression (ODR) by Ervin and Armentrout²⁶ or the isoequilibrium (or isothermal) point method by Bouchoux et al.,¹⁹ has been described. Instead of using two plots to find $\Delta H^\circ_{\text{acid}}(HA_0)$, the isoequilibrium method determines the values of $\Delta H^\circ_{\text{acid}}(HA_0)$ and $\Delta\Delta S^\circ(HA_0, HA_i)$ from a *single* plot in which the linear regressions of $\ln(k_i/k_0)$ vs $\Delta H^\circ_{\text{acid}}(HA_i)$ have converged to a *single* point, called the isoequilibrium point.^{19,27} Problematically, several experiments have shown the existence of multiple isoequilibrium points.²¹ Therefore, a treatment has been developed that forces the convergence of an isoequilibrium point.^{26,28} However, it has been found that results for data analyzed using the isoequilibrium and alternative methods deviate by <0.5 kcal/mol when compared over the same collision energy range.²¹

EXPERIMENTAL SECTION

The MS/MS experiments were performed on a QTrap 4000 (AB SCIEX, Toronto, Canada),³¹ triple quadrupole mass spectrometer. The QTrap offers a linear ion-trap function, which was not used for these experiments. Although the QTrap is a "triple" quadrupole instrument, it contains four quadrupoles. Briefly, the proton-bound heterodimer ions were introduced into the gas phase via electrospray ionization (ESI) of 7.5 μM solutions with respect to both the reference and unknown acids in methanol. Using ESI allowed facile introduction of the proton-bound heterodimers into the gas phase. The infusion rates for these solutions were optimized on a per sample basis and varied from 5 to 40 $\mu\text{L}/\text{min}$. The first quadrupole (Q0) serves as a radio frequency (RF)-only ion guide, and the pressure in this region is $\sim 7 \times 10^{-3}$ Torr of primarily nitrogen gas.³¹ The second quadrupole (Q1), which is capacitively coupled to Q0, is used to select the m/z of the proton-bound heterodimer ions. The ions are then guided into the collision cell (Q2) at multiple collision energies from 5 to 22 eV (lab frame). The collision energy is defined by the dc potential difference between Q0 and Q2. The collision gas pressure is maintained as low as possible at $\sim 6 \times 10^{-3}$ Torr of nitrogen gas. The average number of collisions is estimated to be close to unity. The collision energies are not corrected for perturbations of the true zero of energy, nor are they corrected for multiple collision events. The intensities of ion fragments and undissociated parent ions are monitored with the third quadrupole (Q3), which is coupled to an electron multiplier.

The kinetic method data were analyzed using the alternative method.²⁵ Statistical analysis of the data was performed using Igor Pro (WaveMetrics, Inc.; Lake Oswego, OR, U.S.A.), which implements the freely available software package, ODR-PACK95.³² The first plots of $\ln([A_i^-]/[A_0^-])$ vs $\Delta H^\circ_{\text{acid}}(HA_i)$ were weighted using ordinary least-squares with respect to the standard deviations of $\ln([A_i^-]/[A_0^-])$ at the 95% confidence

interval. The experimental errors for the acidities of the reference acids, $\Delta H^\circ_{\text{acid}}(\text{HA}_i)$, were not included in the statistical analysis of the linear regressions of the first plots. For the second plots of GA^{APP} vs T_{eff} , weighted ODR was implemented to determine $\Delta\Delta S^\circ$ and $\Delta H^\circ_{\text{acid}}(\text{HA}_0)$ using the curve-fitting function $\text{ODR} = 2$ in Igor Pro, also at the 95% confidence interval. Although we use ODR to weight the linear regressions of the second plots, we are not using the isoequilibrium method described by Ervin and Bouchoux.^{19,26–28} All of the chemicals used in this study were purchased from Sigma-Aldrich (St. Louis, MO, U.S.A.), except for 2-nitropyrrole, 3-nitropyrrole, and 3-nitropyrzazole, which were purchased from Oxchem Corporation (Irwindale, CA, U.S.A.), Acella Pharmaceuticals (San Diego, CA, U.S.A.), and Matrix Scientific (Columbia, SC, U.S.A.), respectively.

THEORETICAL CALCULATIONS

Theoretical calculations were carried out using the Gaussian 09 suite of programs.³³ Hybrid functional calculations at the B3LYP/aug-cc-pVTZ level of theory were used to determine theoretical $\Delta G^\circ_{\text{acid}}$, $\Delta H^\circ_{\text{acid}}$, and $\Delta S^\circ_{\text{acid}}$ values for the unknown nitroazoles investigated in this study. Thermal corrections to entropy and free energy were applied under the rigid-rotor harmonic-oscillator approximation. In addition to reporting theoretical $\Delta G^\circ_{\text{acid}}$ values, we also report $\Delta G^\circ_{\text{acid,experiment}}$ values determined by a combination of theory and experiment where $\Delta G^\circ_{\text{acid,experiment}} = \Delta H^\circ_{\text{acid,experiment}} - T\Delta S^\circ_{\text{acid,theory}}$.

RESULTS

The reference acids used for this study are listed in Table 1. The $\Delta H^\circ_{\text{acid}}$ and $\Delta G^\circ_{\text{acid}}$ values were previously determined

Table 1. Reference Acids

reference acid	literature ^a		theory ^b	
	$\Delta H^\circ_{\text{acid}}$	$\Delta G^\circ_{\text{acid}}$	$\Delta H^\circ_{\text{acid}}$	$\Delta G^\circ_{\text{acid}}$
1: phenylacetic acid	341.5 (± 2.1)	334.5 (± 2.0)	339.8	332.7
2: 3-toluic acid	340.6 (± 2.1)	333.6 (± 2.0)	340.8	332.9
3: benzoic acid	340.2 (± 2.2)	333.1 (± 2.0)	340.0	332.3
4: phenoxyacetic acid	338.0 (± 2.2)	331.0 (± 2.0)	335.8	328.4
5: chloroacetic acid	336.5 (± 2.2)	329.0 (± 2.0)	332.7	325.6
6: 4-(trifluoromethyl) benzoic acid	332.3 (± 2.1)	325.3 (± 2.0)	331.9	324.3
7: 4-cyanobenzoic acid ^c	329.4 (± 2.2)	321.7 (± 2.4)	329.0	321.3
8: 3-nitrobenzoic acid	329.1 (± 2.1)	322.1 (± 2.0)	328.8	321.1
9: 4-nitrobenzoic acid	328.1 (± 2.2)	321.1 (± 2.0)	327.5	319.7
10: salicylic acid	325.5 (± 2.2)	317.8 (± 2.0)	328.0	320.6
11: 3,5-bis(trifluoromethyl) benzoic acid	324.4 (± 2.1)	317.4 (± 2.0)	325.8	318.1

^aValues from the NIST Chemistry WebBook.³⁸ ^bTheoretical calculations were carried out using Gaussian 09 at the B3LYP/aug-cc-pVTZ level of theory, and thermal corrections to entropy and free energy are included under the rigid rotor-harmonic oscillator approximation for $T = 298$ K. ^cThe ΔH° and ΔG° values for 7 were redetermined before use in this experiment using the extended kinetic method with the alternative method for data analysis.

using ion–molecule reaction equilibrium methods.^{10–13} $\Delta H^\circ_{\text{acid}}$ for 7 (4-cyanobenzoic acid) was redetermined for use in this study with the extended kinetic method and the alternative method for data analysis.²⁵ The new value of $\Delta H^\circ_{\text{acid}}(\text{HA}_i) = 329.4 \pm 2.2$ kcal/mol was used for subsequent

experiments in which 7 was employed as a reference; this value agrees with the previously determined value, 327.8 ± 2.1 kcal/mol,³⁴ within experimental error. For its experimental determination, 7 was referenced against the carboxylic acids 5, 6, 8, 9, 10, and 11. Because 7, like the reference acids to which it was compared, is a carboxylic acid, the second plot of GA^{APP} vs T_{eff} is characterized by a line with a small slope, where $\Delta\Delta S^\circ = 0.533 \pm 0.303$ cal/(mol K). This result is expected for proton transfer between functionally and structurally similar anions.

The nitrated azole species in this study were extensive enough in their $\Delta H^\circ_{\text{acid}}(\text{HA}_0)$ values to warrant their pairing with three separate groups of reference acids. 2- and 3-Nitropyrrole were referenced against 1, 2, 3, 4, 5, and 6. 3- and 4-Nitropyrzazole were referenced against 5, 6, 7, 8, and 9. Lastly, 2- and 4-nitroimidazole were referenced against 6, 7, 8, 9, 10, and 11. As shown, there is some overlap between the groups of reference acids and unknown acid pairs.

We collected data for each of the azole acid systems at multiple lab-frame collision energies from ~ 5 –22 eV. The limit on the collision energy range is determined for each experiment by analyzing how smoothly the effective temperature (T_{eff}) rises with respect to the collision energies set by the instrument.²¹ Although the data can also be analyzed in the center-of-mass frame, Armentrout and co-workers reported that converting to the center-of-mass frame does not change the character of the results.²¹ For that reason, we have analyzed the data in the conventional laboratory frame.

The ratios of the product ions, $[A_i^-]/[A_0^-]$, were determined by examining the peak heights of pertinent ions as extracted from MS/MS data. Notably, several of the carboxylic reference acids exhibited a loss of m/z 44 (CO_2) upon using higher collision energies (≥ 14 eV). Additionally, some of the species containing a nitro group ($-\text{NO}_2$) exhibited a loss of m/z 30 (NO). Chloride ion was observed as a secondary product ion when reference acid 5 was used. The intensities of the secondary product ions were accounted for by adding their intensities to the respective primary ion intensities, and no further corrections were made.

Figure 2 shows five plots of $\ln(k_i/k_0)$ vs $\Delta H^\circ_{\text{acid}}(\text{HA}_i)$ for 4-nitropyrzazole and its reference acids at the collision energies 5, 7, 10, 14, and 18 eV. Most reports overlay all regressions onto a single plot, and in an ideal situation the linear regressions of the different collision energies will cross at a single point, known as the isoequilibrium point. However, most extended kinetic method data deviate from a single crossing point,²¹ and the data for this study are no exception. The slope of the linear regression decreases as the collision energy increases from part a to e of Figure 2. This decrease in slope corresponds to an increase in T_{eff} , because slope is proportional to $1/T_{\text{eff}}$. Simultaneously, the x -intercept, indicated by a blue arrow, increases from part a to e of Figure 2, corresponding to an increase in the GA^{APP} term. The two values, GA^{APP} and T_{eff} are plotted in a second graph, shown as Figure 3. Analysis of the y -intercept and slope of the second plot provides values for $\Delta H^\circ_{\text{acid}}(\text{HA}_0)$ and $\Delta\Delta S^\circ(\text{HA}_0, \text{HA}_i)$, as shown by the relationship in eq 2.

Table 2 gives a complete summary of the results of our measurements. The experimental results $\Delta H^\circ_{\text{acid}}(\text{HA}_0)$ were obtained by the alternative method of data analysis. Additionally, $\Delta H^\circ_{\text{acid}}(\text{HA}_0)$ values were theoretically calculated for each nitrated azole. The calculated $\Delta H^\circ_{\text{acid}}(\text{HA}_0)$ values agree with the experimental values within 1 kcal/mol, except for 3-

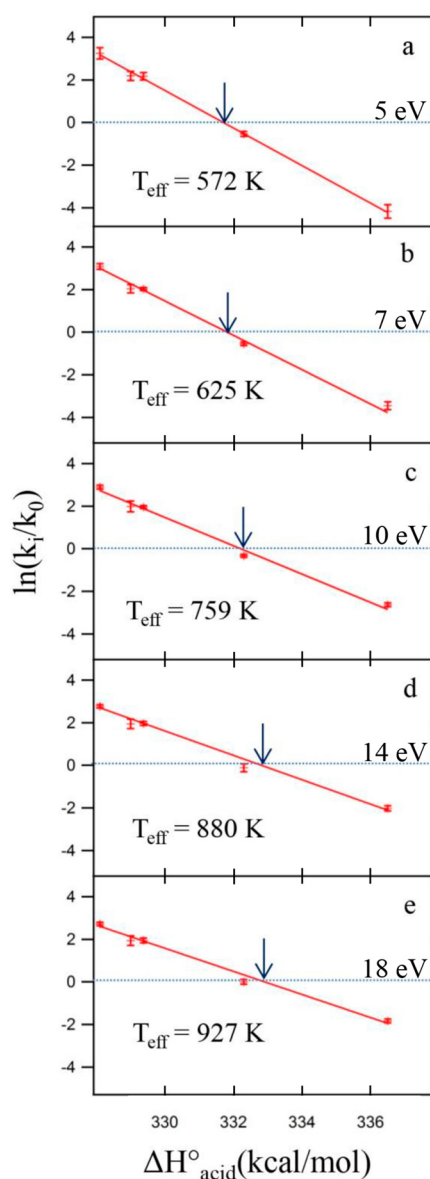


Figure 2. Plots of $\ln(k_i/k_0)$ vs $\Delta H^\circ_{\text{acid}}$ (kcal/mol) for 4-nitropyrazole at the five collision energies 5, 7, 10, 14, and 18 eV (lab frame) for plots a, b, c, d, and e, respectively. As the collision energy increases, the slope ($-1/RT_{\text{eff}}$) becomes less negative and the x -intercept increases; at the x -intercept, $GA^{\text{app}} = \Delta H^\circ_{\text{acid}}$. Note that the $\Delta H^\circ_{\text{acid}}$ values plotted correspond to the reference acids 5, 6, 7, 8, and 9, not to 4-nitropyrazole.

nitropyrazole, which deviates from the experimental value by 1.7 kcal/mol. We also report $\Delta G^\circ_{\text{acid}}(\text{HA}_0)$ values for the unknowns; these values were determined by calculating $T\Delta S^\circ_{\text{acid}}$ ($T = 298$ K) and subtracting the result from the experimental $\Delta H^\circ_{\text{acid}}$ values ($\Delta G^\circ_{\text{acid,experiment}} = \Delta H^\circ_{\text{acid,experiment}} - T\Delta S^\circ_{\text{acid,theory}}$). This approach provides reasonably accurate $\Delta G^\circ_{\text{acid}}$ values because the entropic contribution to the free energy of deprotonation can be calculated with reasonable certainty. The absolute error reported for the $\Delta G^\circ_{\text{acid}}$ values is ± 2.4 kcal/mol because of the added uncertainty introduced by the calculation.

In addition to the experimental kinetic method measurements, we performed a theoretical investigation to determine the $\Delta H^\circ_{\text{acid}}(\text{HA})$, $\Delta G^\circ_{\text{acid}}(\text{HA})$, and electron affinity (EA) values for 24 azolate and nitrated-azolate species. These results

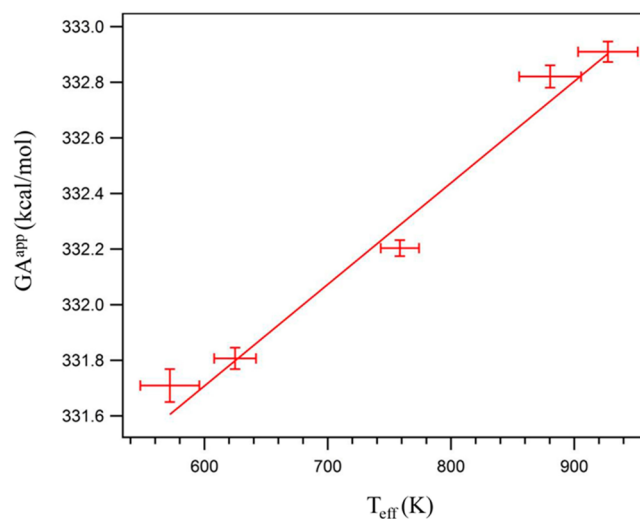


Figure 3. Plot of GA^{app} vs T_{eff} values for 4-nitropyrazole, which were determined from the data in Figure 2. The points are weighted in both the dependent and independent variables at the 95% confidence interval using ODR; the error bars represent two standard deviations of the data. The slope and y -intercept of the weighted line give values for $\Delta\Delta S^\circ$ (3.7 cal/(mol K)) and $\Delta H^\circ_{\text{acid}}$ (329.5 kcal/mol), respectively.

supplement the experimental work by investigating higher-order aza compounds, as well investigating azoles with two nitro groups. The results are presented in Table 3,^{14–16,34–38} which compiles previously determined experimental values, in addition to theoretical values. The theoretical anion proton affinities agree with the experimental measurements within 3 kcal/mol.

DISCUSSION

Recently, Armentrout and co-workers investigated the gas-phase acidities of rigid-planar-monohalogenated phenols using the B3LYP/aug-cc-pVTZ level of theory. (It is noteworthy to mention that they optimized the molecular geometries using a slightly smaller basis set, aug-cc-pVDZ.) Their experimental and theoretical 298 K acidity values present a fairly good correlation, with mean absolute deviations of 2 ± 1 kcal/mol.²¹ To further investigate the correlation between theory and experiment, we calculated the 298 K acidity values for the reference acids used in these studies, and found mean absolute deviations of 1 ± 3 kcal/mol. However, when species containing halogens are removed from the comparison, as well as phenoxyacetic acid, which likely has anharmonic vibrations due to the floppy nature of the etheral, carboxylic moiety, the correlation is improved to 0 ± 3 kcal/mol. Therefore, computations at the B3LYP/aug-cc-pVTZ level of theory should appropriately predict the gas-phase acidities of the rigid-planar organic molecules investigated in Table 3 with a reasonable uncertainty.

The aza substituent effect was investigated previously by Taft et al.³⁶ Upon finding that imidazole is a stronger acid than pyrazole, they argued that the lone pair repulsion from the ring-nitrogen atoms on the pyrazole anion destabilizes it, making pyrazole a weaker acid than imidazole. Additionally, they report the conjugate bases of pyrazole and imidazole to be more stable than pyrrole by 4.8 and 8.4 kcal/mol, respectively. The work of Taft et al. exploits $\Delta G^\circ_{\text{acid}}(\text{HA})$, while our work examines $\Delta H^\circ_{\text{acid}}(\text{HA})$. However, relative differences between these two

Table 2. Results

nitrated azole	E_{coll} (eV)	T_{eff} (K)	experiment			theory ^c		
			$\Delta H_{\text{acid}}^{\circ a}$ (kcal/mol)	$\Delta \Delta S^{\circ a}$ [cal/(mol K)]	$\Delta G_{\text{acid}}^{\circ b}$ (kcal/mol)	$\Delta H_{\text{acid}}^{\circ}$ (kcal/mol)	$\Delta G_{\text{acid}}^{\circ}$ (kcal/mol)	$T\Delta S_{\text{acid}}^{\circ d}$ (kcal/mol)
2-nitropyrrole	6–18	435–645	337.0 (± 2.2)	2.3 (± 0.2)	329.4 (± 2.4)	336.0	328.4	7.6
3-nitropyrrole	6–18	560–880	335.8 (± 2.2)	3.2 (± 0.2)	328.4 (± 2.4)	334.1	326.6	7.4
3-nitropyrzazole	6–18	690–1010	330.5 (± 2.2)	4.7 (± 0.3)	323.1 (± 2.4)	331.2	323.7	7.4
4-nitropyrzazole	5–18	570–930	329.5 (± 2.2)	3.7 (± 0.3)	322.0 (± 2.4)	330.0	322.5	7.5
2-nitroimidazole	6–22	500–735	327.4 (± 2.2)	1.9 (± 0.3)	319.7 (± 2.4)	328.2	320.5	7.7
4-nitroimidazole	6–22	625–975	325.0 (± 2.2)	3.0 (± 0.3)	317.6 (± 2.4)	325.8	318.4	7.4

^aThe values $\Delta H_{\text{acid}}^{\circ}$ and $\Delta \Delta S^{\circ}$ were determined using the alternative method for extended kinetic method data analysis. ODR was used to weight the two values in the second plot. The errors for $\Delta H_{\text{acid}}^{\circ}$ arise from the uncertainties of the reference acids. The experimental precision from the ODR statistical treatment of the data at the 95% confidence interval is much better ($\leq \pm 0.4$ kcal/mol) than the absolute error. ^b $\Delta G_{\text{acid,experiment}}^{\circ}$ was determined by a combination of theory and experiment where ($\Delta G_{\text{acid,experiment}}^{\circ} = \Delta H_{\text{acid,experiment}}^{\circ} - T\Delta S_{\text{acid,theory}}^{\circ}$). ^cTheoretical calculations were carried out using Gaussian 09 at the B3LYP/aug-cc-pVTZ level of theory, and thermal corrections to entropy and free energy are included under the rigid rotor-harmonic oscillator approximation. ^d $T = 298$ K.

thermodynamic properties are comparable because the entropic contribution is roughly constant with $T\Delta S$ usually changing by < 1 kcal/mol for any given pair of acids. Our work expands these observations and explores trends in nitration effects. On the basis of the difference in acidity between 2- and 3-nitropyrrole and pyrrole, 3- and 4-nitropyrzazole and pyrazole, and 2- and 4-nitroimidazole and imidazole, we report that, when a nitro group is substituted onto an azole, it increases the acidity by 23.5 ± 1.9 kcal/mol at the 95% confidence interval.^{14–16} This is in excellent agreement with the experimentally determined differences in acidity between benzene and nitrobenzene, 24.2 kcal/mol.^{18,39}

As stated in the results, the anions under investigation for this study were sufficiently different in $\Delta H_{\text{acid}}^{\circ}(\text{HA}_0)$ values to require their evaluation with three separate groups of reference acids. Although we report the absolute error for each measured $\Delta H_{\text{acid}}^{\circ}(\text{HA}_0)$ as ± 2.2 kcal/mol, the relative difference in acidity between each pair is 1.2 ± 0.3 kcal/mol for 2-nitropyrrole and 3-nitropyrrole, 1.0 ± 0.7 kcal/mol for 3-nitropyrzazole and 4-nitropyrzazole, and 2.4 ± 0.6 kcal/mol for 2-nitroimidazole and 4-nitroimidazole. Relative uncertainties are reported at the 95% confidence interval (2σ). This ordering is reinforced because the acidities of each pair were determined using the same reference acids. Furthermore, the experiments are much more precise (± 0.4 kcal/mol) than the absolute uncertainty (± 2.2 kcal/mol). This allows us to arrange with confidence the proposed azoles in order of increasing acidity as 2-nitropyrrole, 3-nitropyrrole, 3-nitropyrzazole, 4-nitropyrzazole, 2-nitroimidazole, and 4-nitroimidazole, which have $\Delta H_{\text{acid}}^{\circ}$ (kcal/mol) values of 337.0, 335.8, 330.5, 329.5, 327.4, and 325.0, respectively. To provide some context, other common anions of ionic liquids including Cl^- , Br^- , CF_3SO_3^- , and NTf_2^- have $\Delta H_{\text{acid}}^{\circ}$ (kcal/mol) values of 333.40, 323.54, 305.4, and 293.3, respectively.

The differences in acidity among the nitrated azoles can be attributed to nitrogen atom and nitro group placement. Imidazole is more acidic than pyrazole because pyrazole is destabilized by the adjacent placement of the two nitrogen atoms. A similar destabilization occurs when a nitro group is located adjacent to a ring-nitrogen atom. The optimized equilibrium geometries for each of the six nitrated azoles experimentally investigated in this study yield planar molecules. Therefore, the oxygen atoms of the nitro groups are in close proximity to the neighboring ring atoms. This orientation introduces a region of high electron density in proximity to ring

atoms that are adjacent to the nitro group. Understanding the geometries helps us explain the relative ordering between the sub groups. 2-Nitropyrrole is a weaker acid than 3-nitropyrrole because the electron-dense region of the oxygen atom is repulsive toward the electron-dense region of the ring-nitrogen atom. This same argument holds for the difference in acidity between 3- and 4-nitropyrzazole; 4-nitropyrzazole is more acidic than 3-nitropyrzazole because 3-nitropyrzazole faces a higher degree of electron repulsion when the electron-dense oxygen atom is in close proximity to the electron-dense ring-nitrogen atom. Lastly, the difference in acidity between 2- and 4-nitroimidazole is more pronounced because the nitro group of 2-nitroimidazole is placed between two ring-nitrogen atoms, resulting in greater electron density overlap. In summary, when a nitro group is placed on an azole ring adjacent to a ring-nitrogen atom, it will destabilize the anion by 1.1 ± 0.3 kcal/mol as compared to the isomer with the nitro group located away from the ring-nitrogen atom.

A few more trends are evident from the additional theoretical investigation, which are consistent with our chemical intuition. First, for higher-order aza substitution, molecules of higher acidity are produced. Second, as the number of nitro groups on the molecule increases, stronger acids are generated. The electron-withdrawing properties of the ring-nitrogen atoms and the nitro groups stabilize the additional electronic charge of the anion, allowing the parent molecule to more easily lose a proton. Again, we found within the dinitro compounds that the nitro group placement can affect the stability of the anion. Placing the nitro groups adjacent to each other will decrease the anion's stability by ~ 2 kcal/mol. (See the difference between 2,3- and 2,4-dinitropyrrole and 2,4- and 4,5-dinitroimidazole.) While this result is consistent with an increase in electrostatic repulsion, spatial constraint issues are also contributing, i.e., 2,4-dinitropyrrole and 2,4-dinitroimidazole are planar while our calculations show that the nitro-group–oxygen atoms of 2,3-dinitropyrrole and 4,5-dinitroimidazole are outside of the molecular plane. Finally, as the acidity of the molecule increases, the electron binding energy of the conjugate base, or anion, also increases. Both of these trends indicate an increase in the stability of the anion.

CONCLUSION

We have employed the extended kinetic method with the alternative method of data analysis to determine $\Delta H_{\text{acid}}^{\circ}$ for six nitrated-azole compounds. The success of this work is

Table 3. Experimental and Theoretical Thermochemical Properties of Nitrated Azoles

azole	experiment			theory ^a		
	$\Delta H_{\text{acid}}^{\circ b,c}$ (kcal/mol)	$\Delta G_{\text{acid}}^{\circ c,d}$ (kcal/mol)	EA ^e (eV)	$\Delta H_{\text{acid}}^{\circ b,c}$ (kcal/mol)	$\Delta G_{\text{acid}}^{\circ c,d}$ (kcal/mol)	EA ^e (eV)
pyrrole	359.54 (± 0.25) ¹⁴ 358.6 (± 2.2) ³⁵	350.9 (± 2.0) ¹⁴	2.145 (± 0.010) ¹⁴	360.1	352.6	2.104
2-nitropyrrole	337.0 (± 2.2) ^f			336.0	328.4	3.436
3-nitropyrrole	335.8 (± 2.2) ^f			334.1	326.6	3.416
2,3-dinitropyrrole				317.2	309.8	4.165
2,4-dinitropyrrole				315.0	307.4	4.487
2,5-dinitropyrrole				315.2	307.5	4.501
pyrazole	353.6 (± 2.4) ¹⁶	346.4 (± 2.3) ¹⁶	2.938 (± 0.005) ¹⁶	355.7	348.1	2.908
3-nitropyrazole	330.5 (± 2.2) ^f			(N1)331.2 (N2)331.7	(N2)323.7 (N2)324.0	4.154
4-nitropyrazole	329.5 (± 2.2) ^f			330.0	322.5	4.220
3,4-dinitropyrazole				(N1)313.1 (N2)312.1	(N1)306.4 (N2)304.6	5.011
3,5-dinitropyrazole				311.3	303.7	5.125
imidazole	349.93 (± 0.72) ¹⁵ 350.1 (± 2.1) ³⁶	342.60 (± 0.40) ¹⁵ 342.8 (± 2.0) ³⁶	2.613 (± 0.006) ¹⁵	350.8	343.3	2.562
2-nitroimidazole	327.4 (± 2.2) ^f			328.2	320.5	3.789
4-nitroimidazole	325.0 (± 2.2) ^f			(N1)325.8 (N3)326.6	(N1)318.4 (N3)319.0	3.865
2,4-dinitroimidazole				(N1)307.9 (N3)307.3	(N1)300.1 (N3)299.5	4.836
4,5-dinitroimidazole				309.6	302.5	4.851
1,2,3-triazole	(N2)346.4 (± 2.1) ³⁷	(N2)339.1 (± 2.0) ³⁷	3.447 (± 0.004) ³⁸	(N1)343.2 (N2)346.9	(N1)335.6 (N2)339.3	3.420
4-nitro-1,2,3-triazole				(N1)319.4 (N2)322.3 (N3)318.5	(N1)311.9 (N2)314.8 (N3)310.9	4.626
4,5-dinitro-1,2,3-triazole				(N1)301.5 (N2)304.9	(N1)294.1 (N2)297.9	5.377
1,2,4-triazole	(N1)344.2 (± 2.1) ³⁴	(N1)336.9 (± 2.0) ³⁴		(N1)345.2 (N4)339.4	(N1)337.7 (N4)331.9	3.367
3-nitro-1,2,4-triazole				(N1)321.8 (N2)322.6 (N4)317.2	(N1)314.6 (N2)314.8 (N4)309.5	4.503
3,5-dinitro-1,2,4-triazole				(N1)303.1 (N4)298.1	(N1)295.4 (N4)290.0	5.428
tetrazole	(N1)333.7 (± 2.1) ³⁴	(N1)326.4 (± 2.0) ³⁴		(N1)331.1 (N2)333.0	(N1)323.5 (N2)325.4	4.070
nitrotetrazole				(N1)308.4 (N2)310.2	(N1)300.6 (N2)302.9	5.172

^aTheoretical values calculated using B3LYP/aug-cc-pVTZ methods. $\Delta H_{\text{acid}}^{\circ}$ and $\Delta G_{\text{acid}}^{\circ}$ are reported at 298 K using the rigid-rotor harmonic-oscillator approximation. EA are reported at 0 K including zero-point energies. ^bProton affinity of the anion. ^cThe nitrogen-atom acid site is indicated in parentheses for both experimental and theoretical anion proton affinities and gas-phase acidities. ^dGas-phase acidity. ^eElectron binding energy of the anion (electron affinity of the corresponding neutral radical). ^fExperimental values determined from this work.

attributed to employing reliable reference acids of similar function and structure. The reference acids used were similar in acidity (± 6 kcal/mol) to the acidity of the nitrated azoles, and the reference acids' acidity range encompassed the acidity of the nitrated azoles. The results of this experiment elucidate trends in the mononitration of pyrrole, pyrazole, and imidazole. We conclude that the pertinent anions of this study are very stable, and they should be capable of generating robust ionic liquids. In addition, previous studies have shown that the basicity of an ionic liquid is dominated by the gas-phase basicity of the anion.^{8,40} Therefore, these experimental measurements provide insight into the Lewis-base properties of ionic liquids in which the anions of this study are employed.

Furthermore, 4-nitroimidazole, the strongest acid of this study, has already found use as the anionic component of ionic liquids in a recent study of azole-based ionic liquids conducted by Rogers and co-workers.⁹ For future work, it would be interesting to investigate the gas-phase acidity of the remaining molecules of Rogers' report including the nitrated triazoles, tetrazoles, benzoimidazoles, and benzotriazoles. In addition to our experimental work, we have computationally determined the gas-phase acidity of five other azolate anions found in Rogers' study including 2,4-dinitroimidazole; 4,5-dinitroimidazole; 4-nitro-1,2,3-triazole; 3,5-dinitro-1,2,4-triazole; and tetrazole ($\Delta H_{\text{acid}}^{\circ} = 307, 310, 319, 298,$ and 331 kcal/mol, respectively, for the most acidic sites). These results suggest that most of the azolate-based ionic liquids should have a

reasonably low melting point while maintaining thermal stability up to ~ 200 °C. From our investigation, no clear trend between acidity and ionic liquid melting point is revealed. Conversely, the thermal stability of the ionic liquid pair increases with the gas-phase stability of the anion.⁹

Finally, these studies indicate that the addition of a nitro group to an aromatic ring will increase the compound's acidity/anionic stability by 23.5 ± 1.9 kcal/mol. Moreover, these molecules are marginally destabilized by 1.1 ± 0.3 kcal/mol when the nitro group is placed adjacent to a ring-nitrogen atom. By understanding these trends, researchers will have greater control over the thermodynamic properties of novel ionic liquids.

AUTHOR INFORMATION

Corresponding Author

*E-mail: Veronica.Bierbaum@colorado.edu. Phone: 303-492-7081.

Notes

The authors declare no competing financial interest.

ACKNOWLEDGMENTS

The authors gratefully acknowledge support of this work by the Air Force Office of Scientific Research (FA9550-12-1-0125) and the National Science Foundation (CHE-1300886). We are grateful to the Extreme Science and Engineering Discovery Environment (XSEDE), which is supported by the National Science Foundation (ACI-1053575). Any opinion, findings, and conclusions expressed in this material are those of the authors and do not necessarily reflect the views of the National Science Foundation. We also thank the reviewers of this manuscript for their useful comments that have increased the quality of this paper.

REFERENCES

- (1) Reedijk, J. Pyrazoles and imidazoles as ligands. Part I. Some simple metal(II) perchlorates and tetrafluoroborates solvated by neutral pyrazole and imidazole. *Recl. Trav. Chim. Pays-Bas* **1969**, *88*, 1451–1470.
- (2) Angell, C. A.; Ansari, Y.; Zhao, Z. F. Ionic liquids: past, present and future. *Faraday Discuss.* **2011**, *154*, 9–27.
- (3) Jodry, J. J.; Mikami, K. Ionic liquids. In *Green reaction media in organic synthesis*, 1st ed.; Mikami, K., Ed.; Blackwell Publishing Ltd.: Kundli, India, 2005; pp 9–54.
- (4) Wishart, J. F. Energy applications of ionic liquids. *Energy Environ. Sci.* **2009**, *2*, 956–961.
- (5) Armand, M.; Endres, F.; MacFarlane, D. R.; Ohno, H.; Scrosati, B. Ionic-liquid materials for the electrochemical challenges of the future. *Nat. Mater.* **2009**, *8*, 621–629.
- (6) Schneider, S.; Hawkins, T.; Rosander, M.; Vaghjiani, G.; Chambreau, S.; Drake, G. Ionic liquids as hypergolic fuels. *Energy Fuels* **2008**, *22*, 2871–2872.
- (7) Chin, Y. H.; Dressler, R. A. Ionic Liquids for Space Propulsion. In *Ionic liquids IV: not just solvents anymore*; Brennecke, J. F., Rogers, R. D., Seddon, K. R., Eds.; American Chemical Society: Washington, DC, 2007; Vol. 975, pp 138–160.
- (8) Katritzky, A. R.; Singh, S.; Kirichenko, K.; Holbrey, J. D.; Smiglak, M.; Reichert, W. M.; Rogers, R. D. 1-Butyl-3-methylimidazolium 3,5-dinitro-1,2,4-triazolate: a novel ionic liquid containing a rigid, planar energetic anion. *Chem. Commun.* **2005**, *1*, 868–870.
- (9) Smiglak, M.; Hines, C. C.; Wilson, T. B.; Singh, S.; Vincek, A. S.; Kirichenko, K.; Katritzky, A. R.; Rogers, R. D. Ionic liquids based on azolate anions. *Chem.—Eur. J.* **2010**, *16*, 1572–1584.
- (10) Cai, J. F.; Topsom, R. D.; Headley, A. D.; Koppel, I.; Mishima, M.; Taft, R. W.; Veji, S. Acidities of substituted acetic acids. *J. Mol. Struct.: THEOCHEM* **1988**, *45*, 141–146.
- (11) Taft, R. W.; Topsom, R. D. The nature and analysis of substituent effects. *Prog. Phys. Org. Chem.* **1987**, *16*, 1–83.
- (12) McMahon, T. B.; Kebarle, P. Intrinsic acidities of substituted phenols and benzoic-acids determined by gas-phase proton-transfer equilibria. *J. Am. Chem. Soc.* **1977**, *99*, 2222–2230.
- (13) Caldwell, G.; Renneboog, R.; Kebarle, P. Gas-phase acidities of aliphatic carboxylic-acids based on measurements of proton-transfer equilibria. *Can. J. Chem.: Rev. Can. Chim.* **1989**, *67*, 611–618.
- (14) Gianola, A. J.; Ichino, T.; Hoenigman, R. L.; Kato, S.; Bierbaum, V. M.; Lineberger, W. C. Thermochemistry and electronic structure of the pyrrolyl radical. *J. Phys. Chem. A* **2004**, *108* (46), 10326–10335.
- (15) Gianola, A. J.; Ichino, T.; Hoenigman, R. L.; Kato, S.; Bierbaum, V. M.; Lineberger, W. C. Photoelectron spectra and ion chemistry of imidazolide. *J. Phys. Chem. A* **2005**, *109*, 11504–11514.
- (16) Gianola, A. J.; Ichino, T.; Kato, S.; Bierbaum, V. M.; Lineberger, W. C. Thermochemical studies of pyrazolide. *J. Phys. Chem. A* **2006**, *110*, 8457–8466.
- (17) Eyet, N.; Bierbaum, V. M. Gas-phase acidities of thiocarboxylic acids. *Int. J. Mass Spectrom.* **2007**, *265*, 267–270.
- (18) Cheng, X.; Grabowski, J. J. Gas-phase acidity of nitrobenzene from flowing afterglow bracketing studies. *Rapid Commun. Mass Spectrom.* **1989**, *3*, 34–36.
- (19) Bouchoux, G.; Sablier, M.; Berruyer-Penaud, F. Obtaining thermochemical data by the extended kinetic method. *J. Mass Spectrom.* **2004**, *39*, 986–997.
- (20) Cooks, R. G.; Koskinen, J. T.; Thomas, P. D. Special feature: Commentary—The kinetic method of making thermochemical determinations. *J. Mass Spectrom.* **1999**, *34*, 85–92.
- (21) Bourgoin-Voillard, S.; Afonso, C.; Lesage, D.; Zins, E. L.; Tabet, J. C.; Armentrout, P. B. Critical evaluation of kinetic method measurements: Possible origins of nonlinear effects. *J. Am. Soc. Mass Spectrom.* **2013**, *24*, 365–380.
- (22) Wenthold, P. G. Determination of the proton affinities of bromo- and iodoacetonitrile using the kinetic method with full entropy analysis. *J. Am. Soc. Mass Spectrom.* **2000**, *11*, 601–605.
- (23) Cheng, X. H.; Wu, Z. C.; Fenselau, C. Collision energy-dependence of proton-bound dimer dissociation—entropy effects, proton affinities, and intramolecular hydrogen-bonding in protonated peptides. *J. Am. Chem. Soc.* **1993**, *115*, 4844–4848.
- (24) Nold, M. J.; Cerda, B. A.; Wesdemiotis, C. Proton affinities of the N- and C-terminal segments arising upon the dissociation of the amide bond in protonated peptides. *J. Am. Soc. Mass Spectrom.* **1999**, *10*, 1–8.
- (25) Armentrout, P. B. Entropy measurements and the kinetic method: A statistically meaningful approach. *J. Am. Soc. Mass Spectrom.* **2000**, *11*, 371–379.
- (26) Ervin, K. M.; Armentrout, P. B. Systematic and random errors in ion affinities and activation entropies from the extended kinetic method. *J. Mass Spectrom.* **2004**, *39*, 1004–1015.
- (27) Bouchoux, G.; Djazi, F.; Gaillard, F.; Vierzetz, D. Application of the kinetic method to bifunctional bases MIKE and CID-MIKE test cases. *Int. J. Mass Spectrom.* **2003**, *227*, 479–496.
- (28) Bouchoux, G. Evaluation of the protonation thermochemistry obtained by the extended kinetic method. *J. Mass Spectrom.* **2006**, *41*, 1006–1013.
- (29) Vekey, K. Internal energy effects in mass spectrometry. *J. Mass Spectrom.* **1996**, *31*, 445–463.
- (30) Drahos, L.; Vekey, K. Special feature: Commentary—How closely related are the effective and the real temperature. *J. Mass Spectrom.* **1999**, *34*, 79–84.
- (31) Hager, J. W. A new linear ion trap mass spectrometer. *Rapid Commun. Mass Spectrom.* **2002**, *16*, 512–526.
- (32) Boggs, P. T.; Donaldson, J. R.; Byrd, R. H.; Schnabel, R. B. ODRPACK95—software for weighted orthogonal distance regression. *ACM Trans. Math. Software* **1992**, *15*, 348–364.

(33) Frisch, M. J.; Trucks, G. W.; Schlegel, H. B.; Scuseria, G. E.; Robb, M. A.; Cheeseman, J. R.; Scalmani, G.; Barone, V.; Mennucci, B.; Peterson, G. A. et al. *Gaussian 09*, Revision A.1; Gaussian, Inc.: Wallingford, CT, 2009.

(34) Lias, S. G.; Bartmess, J. E.; Liebman, J. F.; Holmes, J. L.; Mallard, W. G. NIST Chemistry WebBook. In *Ion Energetics Data* [Online]; Lindstrom, P. J., Mallard, W. G., Eds.; National Institute of Standards and Technology: Gaithersburg, MD, 2014 (accessed September 12, 2014).

(35) Bartmess, J. E.; Scott, J. A.; McIver, R. T. Scale of acidities in the gas phase from methanol to phenol. *J. Am. Chem. Soc.* **1979**, *101*, 6046–6056.

(36) Taft, R. W.; Anvia, F.; Taagepera, M.; Catalan, J.; Elguero, J. Electrostatic proximity effects in the relative basicities and acidities of pyrazole, imidazole, pyridazine, and pyrimidine. *J. Am. Chem. Soc.* **1986**, *108*, 3237–3239.

(37) Catalan, J.; Claramunt, R. M.; Elguero, J.; Laynez, J.; Menendez, M.; Anvia, F.; Quiñan, J. H.; Taagepera, M.; Taft, R. W. Basicity and acidity of azoles—The annelation effect in azoles. *J. Am. Chem. Soc.* **1988**, *110*, 4105–4111.

(38) Ichino, T.; Andrews, D. H.; Rathbone, G. J.; Misaizu, F.; Calvi, R. M. D.; Wren, S. W.; Kato, S.; Bierbaum, V. M.; Lineberger, W. C. Ion chemistry of 1H-1,2,3-triazole. *J. Phys. Chem. B* **2008**, *112*, 545–557.

(39) Gunion, R. F.; Gilles, M. K.; Polak, M. L.; Lineberger, W. C. Ultraviolet photoelectron-spectroscopy of the phenide, benzyl and phenoxide anions, with ab initio calculations. *Int. J. Mass Spectrom. Ion Process.* **1992**, *117*, 601–620.

(40) Crowhurst, L.; Mawdsley, P. R.; Perez-Arlandis, J. M.; Salter, P. A.; Welton, T. Solvent–solute interactions in ionic liquids. *Phys. Chem. Chem. Phys.* **2003**, *5*, 2790–2794.